Neuron, Vol. 39, 961–973, September 11, 2003, Copyright ©2003 by Cell Press

$GABA_A$ Receptors at Hippocampal Mossy Fibers

Arnaud Ruiz,[1,3] Ruth Fabian-Fine,[2] Ricardo Scott,[1] Matthew C. Walker,[1] Dmitri A. Rusakov,[1] and Dimitri M. Kullmann[1,*]

[1]Department of Clinical and Experimental Epilepsy
Institute of Neurology
University College London
London, WC1N 3BG
United Kingdom

[2]Department of Psychology and Neuroscience
Institute
Dalhousie University
Halifax, Nova Scotia B3H 4H7
Canada

Summary

Presynaptic $GABA_A$ receptors modulate synaptic transmission in several areas of the CNS but are not known to have this action in the cerebral cortex. We report that $GABA_A$ receptor activation reduces hippocampal mossy fibers excitability but has the opposite effect when intracellular Cl^- is experimentally elevated. Synaptically released GABA mimics the effect of exogenous agonists. $GABA_A$ receptors modulating axonal excitability are tonically active in the absence of evoked GABA release or exogenous agonist application. Presynaptic action potential-dependent Ca^{2+} transients in individual mossy fiber varicosities exhibit a biphasic dependence on membrane potential and are altered by $GABA_A$ receptors. Antibodies against the α_2 subunit of $GABA_A$ receptors stain mossy fibers. Axonal $GABA_A$ receptors thus play a potentially important role in tonic and activity-dependent heterosynaptic modulation of information flow to the hippocampus.

Introduction

Ionotropic GABA receptors contribute to presynaptic modulation of transmission in the mammalian spinal cord (Eccles et al., 1963; Nicoll and Alger, 1979), retina (Lukasiewicz and Werblin, 1994; Tachibana and Kaneko, 1987), posterior pituitary (Saridaki et al., 1989; Zhang and Jackson, 1993), and auditory brainstem (Turecek and Trussell, 2002). Presynaptic $GABA_A$ receptors have also been reported in the ventromedial hypothalamus (Jang et al., 2001). Finally, they have been shown to have an autoreceptor function in the terminals of developing cerebellar interneurons (Pouzat and Marty, 1999). In contrast to the abundance of evidence that presynaptic $GABA_A$ receptors modulate transmission at a variety of subcortical synapses, their role in the cerebral cortex is far from clear. Because $GABA_A$ receptors can mediate rapid signaling, a presynaptic role in the cerebral cortex would have extensive implications for higher information processing. In support of this possibility, $GABA_A$ receptors have been reported to modulate the release of neurotransmitters from synaptosomes (Fassio et al., 1999; Fung and Fillenz, 1983), and seizure-like activity in vitro can initiate ectopic axonal action potentials via $GABA_A$ receptors in Schaffer collaterals (Stasheff et al., 1993). Both of these phenomena are, however, open to alternative interpretations. In particular, $GABA_A$ receptor-mediated responses can be accompanied by efflux of HCO_3^- and K^+ (Voipio and Kaila, 2000). Indeed, extracellular K^+ accumulation has been proposed to account for $GABA_A$ receptor-dependent initiation of ectopic action potentials during epileptiform discharges (Avoli et al., 1998). Thus, there is little compelling evidence that presynaptic $GABA_A$ receptors can directly affect transmitter release at cortical synapses.

Hippocampal mossy fibers are a well-characterized cortical pathway from dentate granule cells to the hippocampus proper. The mossy fiber-CA3 pyramidal cell synapse has been proposed to act as a "conditional detonator" and is critical for information processing within the hippocampus circuitry (Henze et al., 2000). Several presynaptic glutamate and opioid receptors have been shown to modulate mossy fiber transmission (Kamiya et al., 1996; Lanthorn et al., 1984; Scanziani et al., 1997; Schmitz et al., 2001; Vignes et al., 1998; Weisskopf et al., 1993; Yamamoto et al., 1983; Yokoi et al., 1996). Through this means, mossy fiber-CA3 synaptic signaling can be modulated by spillover of neurotransmitters. Notably, GABA depresses mossy fiber transmission via presynaptic metabotropic $GABA_B$ receptors (Min et al., 1998; Vogt and Nicoll, 1999). Prompted by the observation that both metabotropic and ionotropic glutamate receptors can modulate mossy fiber transmission, we asked whether presynaptic ionotropic $GABA_A$ receptors are also present. Such receptors could potentially mediate a more rapid response to changes in extracellular GABA than $GABA_B$ receptors. We report that $GABA_A$ receptors directly modulate mossy fiber excitability, and moreover, that this phenomenon is tonically active at ambient GABA concentrations. Synaptically released GABA also mimics the effect of exogenous $GABA_A$ receptor agonists on mossy fiber excitability. We further show that $GABA_A$ receptors alter Ca^{2+} influx into axonal varicosities. Finally, we provide immunohistochemical evidence at both light and electron microscopic levels for the presence of α_2 subunit-containing $GABA_A$ receptors in mossy fibers.

Results

$GABA_A$ Receptors Modulate Mossy Fiber Excitability

We looked for evidence of functional axonal $GABA_A$ receptors in granule cells by examining the effects of a $GABA_A$ receptor agonist on the excitability of mossy fibers (Kamiya and Ozawa, 2000). We evoked antidromic action potentials via a stimulating electrode positioned in stratum lucidum in acute hippocampal slices, while

*Correspondence: d.kullmann@ion.ucl.ac.uk
[3]Present address: CNRS UMR 5091, Institut François Magendie, 1 rue Camille Saint-Saëns, 33077 Bordeaux Cedex, France.

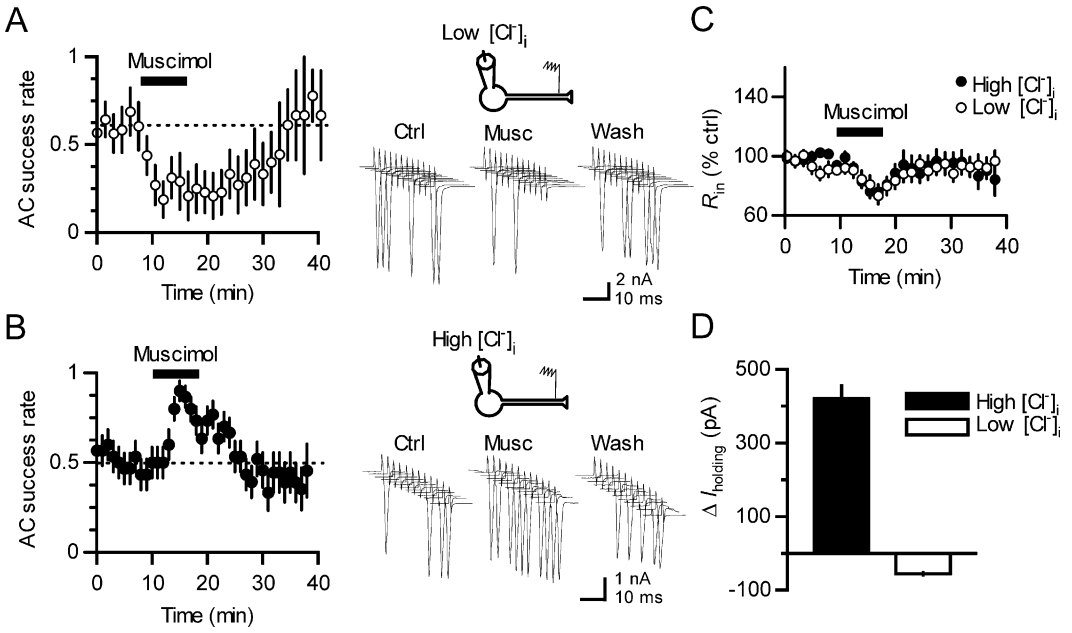

Figure 1. $GABA_A$ Receptors Modulate Hippocampal Mossy Fiber Excitability

(A) Antidromic action current (AC) success rate (mean ± SEM) plotted against time, showing a reduction evoked by bath perfusion of 1 μM muscimol. Right: sample consecutive traces obtained from one neuron before and during muscimol application and following washout.

(B) In granule cells recorded with a high [Cl^-] pipette solution, muscimol increased the success rate for antidromic ACs. Right: sample traces as for (A).

(C) Time course of input resistance following muscimol application in the same cells as shown in (A) and (B).

(D) Bar chart showing opposite changes in somatic holding current after muscimol application.

recording from a granule cell held in voltage clamp at −70 mV with a pipette containing 8 mM Cl^- (close to the concentration estimated in neocortical neurons [Kaila et al., 1993]). AMPA, kainate, NMDA, and $GABA_B$ receptors were blocked pharmacologically. Action potentials were detected as inward action currents (ACs). We lowered the stimulus intensity until stimuli resulted in an AC in 40%–60% of cases. Bath perfusion of a low concentration of the selective $GABA_A$ agonist muscimol (1 μM; EC_{50} for $GABA_A$ receptors, 0.9–8.9 μM; Ebert et al., 1997) reversibly decreased the success rate by 62% ± 12% (mean ± SEM; $p < 0.03$, $n = 8$; Figure 1A). Muscimol had no effect on the AC success rate when suprathreshold stimuli were delivered, implying that it did not act by promoting action potential conduction failure (Verdier et al., 2003). Instead, the results indicate that $GABA_A$ receptors decrease mossy fiber excitability.

Although the effect of muscimol on the AC success rate is consistent with the existence of axonal $GABA_A$ receptors, an alternative possibility is that it acts indirectly by altering the extracellular ionic environment, for instance by promoting K^+ efflux from neighboring neurons via activation of the K^+-Cl^- transporter KCC2 (Payne et al., 1996). We therefore obtained whole-cell recordings from granule cells with a pipette containing a high [Cl^-] solution ($E_{Cl} = +3$ mV), with the goal of shifting the axonal $GABA_A$ reversal potential in a positive direction, without altering the action of muscimol on surrounding neurons and glia. We delayed the application of muscimol until >20 min had elapsed to allow intracellular Cl^- to accumulate. When muscimol was applied, the success rate increased reversibly by 78% ± 8% ($p < 0.01$, $n = 5$; Figure 1B), opposite to the result obtained with a low [Cl^-] recording solution. The fact that manipulation of $[Cl^-]_i$ in only one cell is able to switch the polarity of the effect of muscimol indicates that the phenomenon does not depend critically on changes in extracellular ion concentrations.

Local Agonist Application Implicates Distal Axonal Receptors

Where are the $GABA_A$ receptors that affect axonal excitability? The effects of muscimol obtained with either high or low [Cl^-] pipette solutions were accompanied by a decrease in input resistance (Figure 1C) and opposite changes in somatic holding current (Figure 1D). Because the cell body was kept in voltage clamp, effects of $GABA_A$ receptors on the somatodendritic membrane potential were unlikely to spread to the axonal membrane. However, this does not exclude a role for $GABA_A$ receptors in the axonal initial segment, which may not have been fully clamped. To test whether muscimol altered the action current success rate through a direct effect on axonal receptors, we pressure-applied a low concentration of muscimol (2.5 μM) via a pipette positioned within 50 μm of the stimulating electrode in stratum lucidum and at least 1000 μm from the cell body. Because the dendrites of granule cells are oriented in a direction opposite to that of the mossy fiber, this experimental design precluded activation of receptors in the somatodendritic compartment or in the axonal initial segment. The soma was voltage-clamped with a low [Cl^-] pipette. Pressure application of muscimol in stratum lucidum resulted in a 40% ± 6% decrease in AC success rate

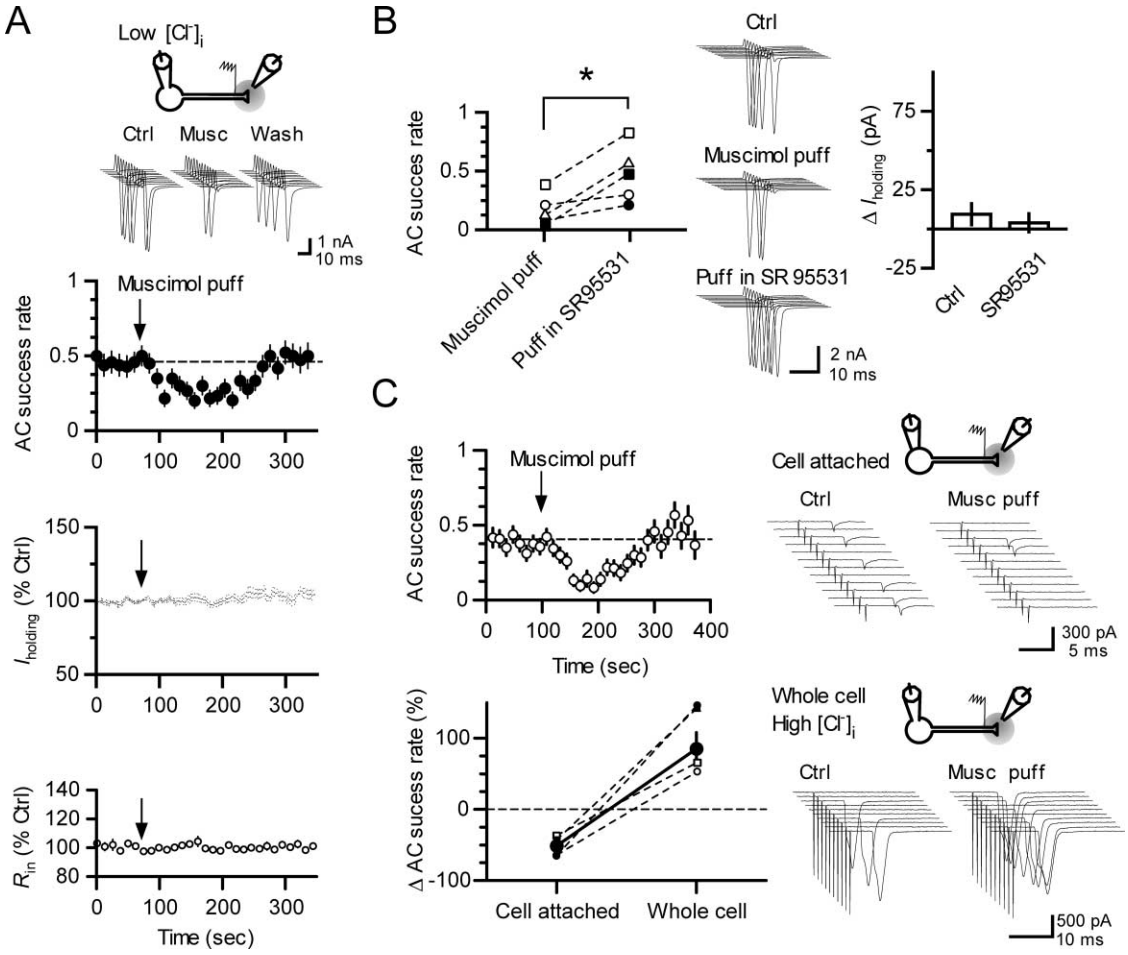

Figure 2. Axonal $GABA_A$ Receptors Modulate Mossy Fiber Excitability

(A) Focal activation of axonal $GABA_A$ receptors with pressure ejection of muscimol (2.5 μM) at the stimulus site in stratum lucidum reversibly depresses the AC success rate (top) but has no effect on the somatic holding current (middle) or the input resistance of granule cells (bottom, average of 6 cells). Sample traces show consecutive ACs taken before (Ctrl), 30 s after pressure application of muscimol (Musc), and following recovery (Wash).

(B) Plot showing that the muscimol-induced depression of AC success rate was prevented by SR95531 (10 μM; $n = 5$). The bar chart at right shows the effect of pressure-applied muscimol on the holding current in the same experiments. The consecutive sample traces were obtained in one cell before (Ctrl), immediately after focal muscimol application (Muscimol puff), and after muscimol in SR95531. *$p < 0.05$.

(C) Modulation of AC success rate by pressure-applied muscimol depends on $[Cl^-]_i$. Top: time course showing the decrease of AC success rate evoked by focal muscimol in cell-attached recordings ($n = 4$). Bottom: graph illustrating the opposite modulation of the AC success rate evoked by focal muscimol application before (Cell attached) and 30 min after break-in with a high chloride pipette (Whole cell). The filled circles show the mean ± SEM for 4 cells. The AC success rate in each case was normalized to the success rate in the absence of muscimol application. Insets show consecutive traces from one cell cell-attached (top) and whole-cell mode (bottom).

($p < 0.01$, $n = 11$ applications in 6 cells), which was accompanied by no change in either the somatic holding current or the input resistance ($p > 0.3$; Figure 2A). This effect indicates that muscimol affected the AC success rate by acting on axonal receptors, electrically close to the site of action potential initiation. We verified that the effect of muscimol was mediated by $GABA_A$ receptors by repeating the agonist application in the presence of the selective antagonist SR95531 (10 μM). This manipulation completely blocked the muscimol-induced depression of the AC success rate ($p < 0.05$; $n = 5$ applications in 4 cells), again with no change in holding current ($p > 0.6$; Figure 2B).

We further tested the hypothesis that axonal $GABA_A$ receptors modulate axonal excitability by applying muscimol locally to the stimulus site while initially recording in cell-attached mode and subsequently in whole-cell mode with a high $[Cl^-]$ solution. During the initial phase of this experiment, pressure ejection of muscimol (2.5 μM) induced a reversible decrease in the AC success rate (Figure 2C, top panel), consistent with the effect obtained with a low $[Cl^-]$ pipette solution (see Figure 2A). Following "break-in," we allowed intracellular Cl^- to equilibrate for 30 min. A second muscimol application caused an increase in AC success rate, opposite to the decrease obtained in the same neurons in cell-attached mode ($p < 0.01$; $n = 4$, Figure 2C, bottom). Thus, $GABA_A$ receptor activation has opposite effects on axonal excitability depending on E_{Cl} within the same granule cell. The finding that $GABA_A$ receptor activation decreases

axonal excitability in cell-attached recordings (and hence in the absence of experimental perturbation of $[Cl^-]_i$) contrasts with the effect of GABA iontophoresis on group I afferent excitability in the spinal cord (Rudomin et al., 1981).

Synaptically Released GABA Mimics the Effect of Exogenous Agonist Application

Although the actions of muscimol indicate that $GABA_A$ receptors are present in mossy fibers, they do not prove that such receptors can respond to the endogenous ligand GABA. We therefore delivered two stimuli with a 25 ms interstimulus interval in order to explore the effect of activating GABAergic terminals in the vicinity of the site of antidromic action potential generation. When the stimulus intensity was adjusted to achieve an almost 100% success rate for the first stimulus, the success rate for the second stimulus was 43% ± 6% ($n = 13$). We then applied the benzodiazepine agonist zolpidem (0.2 μM), which enhances $GABA_A$ receptor affinity in a subtype-dependent manner. This led to a reversible 59% ± 12% decrease in the success rate of the second AC ($p < 0.02$, $n = 6$; Figure 3A). Conversely, blocking $GABA_A$ receptors with SR95531 (10 μM) reversibly increased the success rate for the second stimulus (91% ± 24% increase, $p < 0.03$, $n = 4$; Figure 3B). A similar enhancement of AC success rate was obtained in the presence of another blocker of $GABA_A$ receptors, bicuculline methiodide (123% ± 38% increase, $p < 0.04$, $n = 3$; Figure 3C). These results imply that the reduced axonal excitability following the first stimulus is at least partly due to $GABA_A$ receptor activation.

Circumstantial evidence suggests that mossy fibers themselves may release GABA (Gutierrez and Heinemann, 2001; Sandler and Smith, 1991; Sloviter et al., 1996; Walker et al., 2001). Do presynaptic $GABA_A$ receptors act exclusively as autoreceptors, akin to those reported in cerebellar interneurons (Pouzat and Marty, 1999)? We looked for evidence of remote effects of synaptically released GABA by delivering conditioning stimuli via a second stimulating electrode located in stratum radiatum, designed to activate axons of local interneurons but not the mossy fiber itself. We verified that trains elicited by this electrode did not evoke antidromic action currents in the recorded granule cell. Figure 3D shows that, following high-frequency trains of conditioning stimuli, the success rate for an antidromic action current was reduced by 42% ± 14% of control ($p < 0.02$, $n = 7$). The effect of the conditioning stimuli was blocked by picrotoxin ($p < 0.05$ when compared to results without picrotoxin; $n = 4$; Figure 3E) or SR95531 ($n = 2$, not shown). These results imply that GABA released from other neurons can persist in the extracellular space at a concentration that is able to reduce axon excitability (when recording with a low $[Cl^-]$ pipette) before it is cleared by diffusion and uptake. Whether presynaptic $GABA_A$ receptors on an individual mossy fiber can be activated by GABA released from the same axon cannot be determined from the present results.

Axonal $GABA_A$ Receptors Are Tonically Active in the Absence of Evoked GABA Release

The evidence presented thus far indicates that both exogenous and endogenous $GABA_A$ receptor agonists are able to modulate mossy fiber excitability. Granule cells have recently been shown to express a form of nonsynaptic tonic inhibition mediated by high-affinity $GABA_A$ receptors (Nusser and Mody, 2002; Overstreet and Westbrook, 2001; Stell and Mody, 2002). We therefore asked whether the axonal receptors are also active at ambient GABA levels by looking at the effect of perfusing the selective antagonist SR95531. We examined the antidromic AC success rate obtained with single stimuli delivered at a low frequency, at an intensity just below threshold. Figure 4A (top) shows that, when granule cells were held at −70 mV with a low $[Cl^-]$ pipette, perfusing SR95531 (10 μM) profoundly and reversibly enhanced the antidromic AC success rate in the absence of exogenous agonists ($n = 6$). This implies that tonically active $GABA_A$ receptors reduce mossy fiber excitability. We repeated this experiment with a high $[Cl^-]$ pipette, initially stimulating at an intensity sufficient to obtain near 100% success rate for an AC. SR95531 application in this situation produced a decrease in AC success rate, which partially reversed upon washout ($n = 6$; Figure 4A, bottom). Thus, in agreement with the effects of muscimol application, experimental depolarization of the Cl^- reversal potential reversed the effect of manipulating $GABA_A$ receptors.

We estimated the degree to which mossy fiber excitability can be increased or decreased from baseline by activating or blocking $GABA_A$ receptors. Instead of delivering the antidromic stimulus at a fixed intensity while monitoring the AC success rate, we stepped the stimulus intensity through a cycle and applied muscimol (2 μM) followed by the $GABA_A$ receptor antagonist picrotoxin (100 μM). Figure 4B shows that in all four cells tested (high $[Cl^-]$ pipette, holding potential, −70 mV), muscimol shifted the input-output curve to the left, and picrotoxin applied subsequently shifted it to the right.

Presynaptic $GABA_A$ Receptors Modulate Ca^{2+} Influx into Mossy Fiber Varicosities

Although the above results imply that both exogenous drugs acting at $GABA_A$ receptors and extracellular GABA play a major role in determining the excitability of mossy fibers in response to extracellular stimuli, they say little about the physiological role of axonal $GABA_A$ receptors: action potentials are normally initiated close to the cell body and generally propagate orthodromically with a high safety factor (Cox et al., 2000; Emptage et al., 2001; Koester and Sakmann, 2000; although see Debanne et al., 1997). Can activation of mossy fiber $GABA_A$ receptors affect transmitter release, and if so, how?

It is technically difficult to measure how $GABA_A$ receptors affect orthodromic transmission to postsynaptic targets such as CA3 pyramidal neurons, both because they influence axon recruitment by extracellular stimuli and because of evidence that mossy fibers themselves can release GABA (Gutierrez and Heinemann, 2001; Sandler and Smith, 1991; Sloviter et al., 1996; Walker et al., 2001). Instead, we looked for a possible direct consequence of mossy fiber $GABA_A$ receptors on Ca^{2+} influx into presynaptic boutons. Several lines of evidence suggest that Ca^{2+} influx and transmitter release at mossy fiber synapses are modulated by the presynaptic membrane potential (Geiger and Jonas, 2000; Kamiya

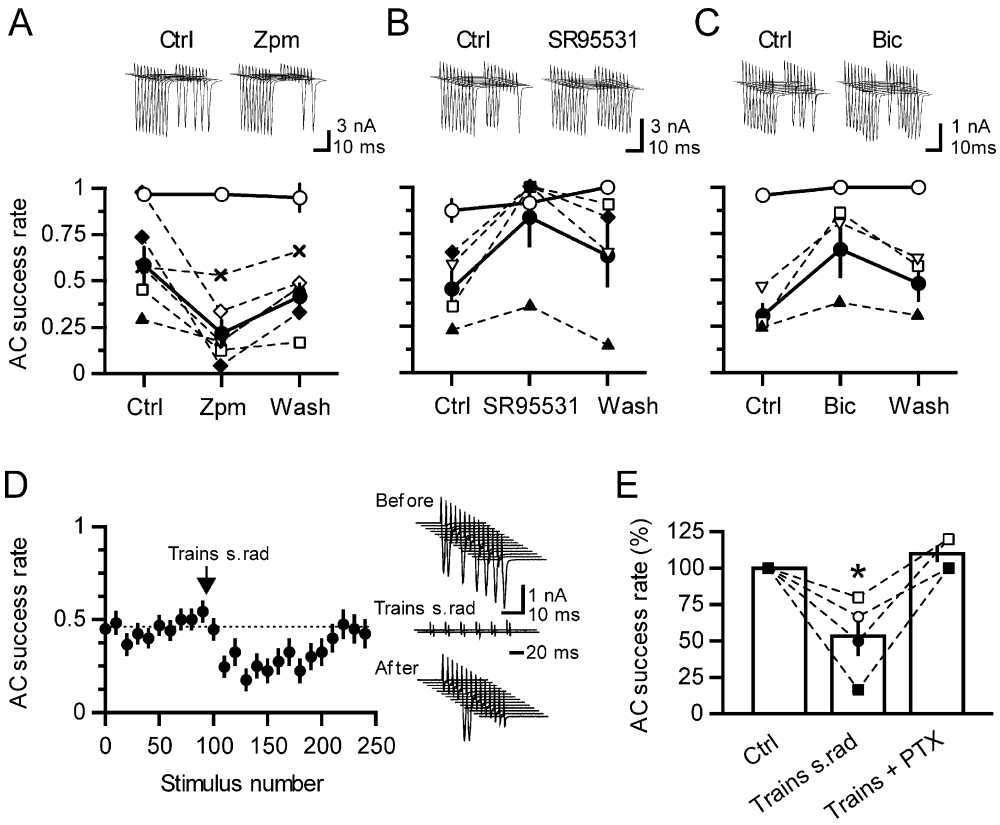

Figure 3. Synaptically Released GABA Activates Presynaptic Receptors

(A–C) AC success rates (mean ± SEM) plotted for the first (open circles, thick connecting lines) and second (closed circles, thick lines) of two stimuli (25 ms interval), while recording from granule cells with a low [Cl^-] pipette solution. The stimulus intensity was adjusted to give a near 100% success rate for the first stimulus. Success rates for the second stimulus in individual experiments are also shown (symbols connected with dashed lines).

(A) Zolpidem (Zpm, 0.2 μM) decreased the antidromic AC success rate for the second pulse without affecting that of the first pulse (n = 6). Inset: sample consecutive traces before and during application of zolpidem.

(B) SR95531 (5 μM) enhanced the success rate for the second pulse (n = 4).

(C) Bicuculline (Bic, 20 μM) also increased the success rate of the second AC (n = 3).

(D) Conditioning trains of stimuli delivered via a second electrode in stratum radiatum (two trains of 5 pulses at 40 Hz, 10 s interval) decreased the AC success rate (n = 7). The conditioning trains themselves did not elicit antidromic ACs. Sample traces: antidromic ACs before (top) and after (bottom) conditioning stimuli (middle).

(E) Summary bar chart of four cells showing a decrease in success rate after trains of stimuli and reversal of this effect by picrotoxin (PTX, 100 μM). *$p < 0.05$.

and Ozawa, 2000; Lauri et al., 2001; Mellor et al., 2002; Schmitz et al., 2001). We therefore applied two-photon excitation microscopy to image fast, action potential-evoked, Ca^{2+}-dependent fluorescence transients (detected with 0.2 mM Fluo-4, at 2 ms sampling) in individual mossy fiber varicosities (Figures 5A–5D). Because the axon could not generally be followed reliably for more than 150–200 μm, the recordings were restricted to relatively proximal varicosities in the dentate hilus (Jackson and Redman, 2003). We held the granule cell in whole-cell voltage clamp mode with a low [Cl^-] pipette and initially examined the effect of changing the holding somatic voltage on the presynaptic Ca^{2+}-dependent fluorescence, both baseline and in response to a suprathreshold antidromic action potential, which was evoked via an extracellular electrode placed in stratum lucidum. (Orthodromic action potentials evoked with 5 ms depolarizing voltage pulses gave identical results.) The action potential was monitored at the granule cell as an AC (Figure 5B). This approach does not allow the local presynaptic membrane potential to be measured simultaneously with the Ca^{2+}-dependent fluorescence. However, if somatic depolarization or hyperpolarization is able to displace the varicosity's potential from rest, changes in Ca^{2+}-dependent fluorescence should reveal the qualitative relationship between the local membrane potential and local Ca^{2+} kinetics.

Depolarizing the soma from −70 mV to −60 mV gave an almost 40% decrease in the size of the Ca^{2+}-dependent fluorescence transient $\Delta F/F$ (fractional fluorescence increment over baseline), which was accompanied by a 19% ± 3% increase in baseline fluorescence F (Figures 5E and 5F). Somatic hyperpolarization, on the other hand, had a biphasic effect on the Ca^{2+}-dependent transient, with an increase (~20%) up to −90 mV and a decrease with larger hyperpolarization, but no effect on baseline F.

In the presence of a high-affinity indicator, the rela-

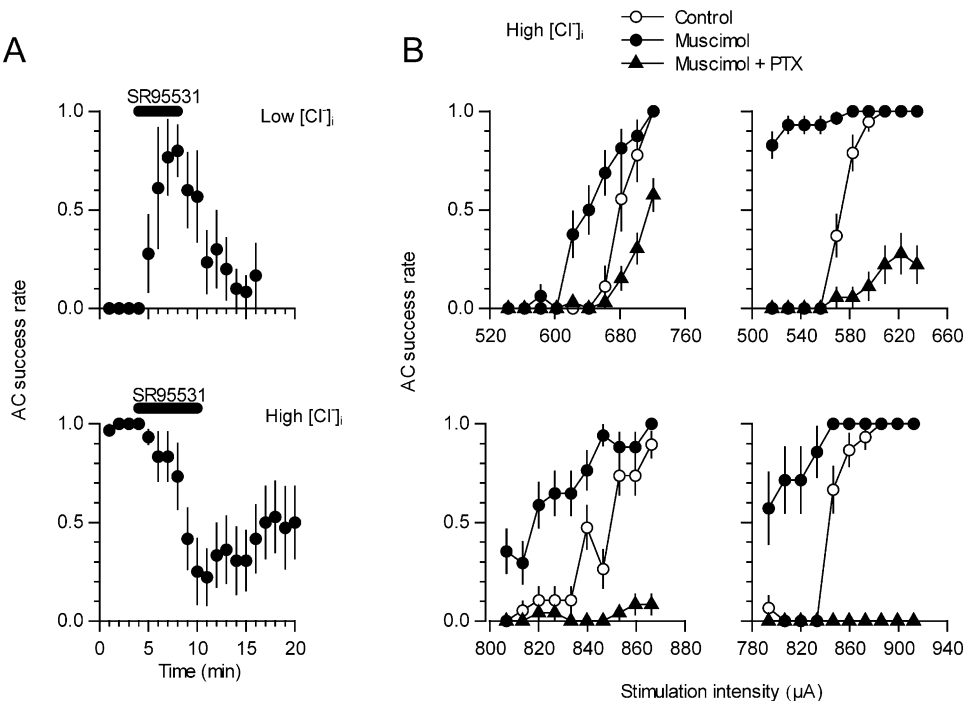

Figure 4. Tonically Active $GABA_A$ Receptors Modulate the Excitability of Mossy Fibers

(A) Top: bath-applied SR95531 (10 μM) increased the success rate for antidromic ACs when cells were recorded with a low [Cl^-] solution ($n = 6$). The stimulation strength was initially set just below threshold for evoking an AC. Bottom: SR95531 had the opposite effect when cells were recorded with a high [Cl^-] solution ($n = 6$).

(B) Input-output curves showing the AC success rate as a function of stimulus intensity for four cells, during a control period, and following successive bath applications of muscimol (2 μM) and picrotoxin (100 μM), when cells were recorded with a high [Cl^-] pipette solution.

tionship between the increment in total intracellular [Ca^{2+}] and $\Delta F/F$ should generally depend on the baseline fluorescence value F (Koester and Sakmann, 2000; Sabatini and Svoboda, 2000). Therefore, to provide a more accurate estimate of the relative magnitude of Ca^{2+} entry with different manipulations that might affect F, we weighted the values of $\Delta F/F$ by changes in F. Kinetic equations predict that, in the conditions of these experiments, this correction should provide >90% accuracy (see Experimental Procedures). (The correction, however, had a relatively minor effect on the relationship between $\Delta F/F$ and holding voltage; red symbols in Figure 5F.) Because there is likely to be appreciable electrotonic attenuation between the soma and the varicosities that were imaged, the "true" relationship between Ca^{2+} influx and local membrane potential prior to action potential arrival is likely to be steeper, and the local voltage corresponding to maximal Ca^{2+} influx cannot be predicted. Nevertheless, this complex dependence upon membrane potential is qualitatively consistent with the biphasic effect of experimental mossy fiber depolarization from a very negative baseline on transmitter release, achieved by applying kainate or elevating $[K^+]_o$ (Schmitz et al., 2001).

We then asked whether tonic $GABA_A$ receptor activation modulates presynaptic Ca^{2+}-dependent fluorescence transients evoked by antidromic stimulation. The cell body was held at −70 mV, corresponding to the steep part of the curve shown in Figure 5F, in order to facilitate reliable detection of an effect of manipulating $GABA_A$ receptors. Muscimol (1 μM) application resulted in a reversible 31% ± 10% increase in the baseline fluorescence ($p < 0.01$, $n = 10$), and this was accompanied by an 18% ± 8% decrease in the action potential-dependent Ca^{2+} fluorescence increment ($\Delta F/F$ corrected for changes in F; $p < 0.05$; Figures 6A–6C). These effects are qualitatively similar to those of somatic depolarization and are consistent with a depolarizing $GABA_A$ reversal potential in granule cells (Misgeld et al., 1986). Although this apparently conflicts with the evidence that $GABA_A$ receptors decrease axonal excitability (Figures 1–4), the action potential threshold is additionally determined by changes in tissue resistivity (and/or axonal impedance) (see Discussion).

We also examined the effect of blocking tonically active $GABA_A$ receptors with 10 μM SR95531. This had no effect on baseline fluorescence but reversibly decreased the action potential-evoked fluorescence transient to 76% ± 9% of baseline ($p < 0.03$, $n = 9$; Figures 6D–6F; $\Delta F/F$ corrected for changes in F). This result implies that removal of tonic activation of presynaptic $GABA_A$ receptors decreases the Ca^{2+} stimulus for exocytosis. This effect is consistent with that of hyperpolarization from a starting point near the maximum of the biphasic relationship between $\Delta F/F$ and voltage.

α_2 Subunit-Containing $GABA_A$ Receptors Are Located to Mossy Fibers

Where are the $GABA_A$ receptors that modulate axon excitability and Ca^{2+} influx into mossy fibers? α_1 and α_2

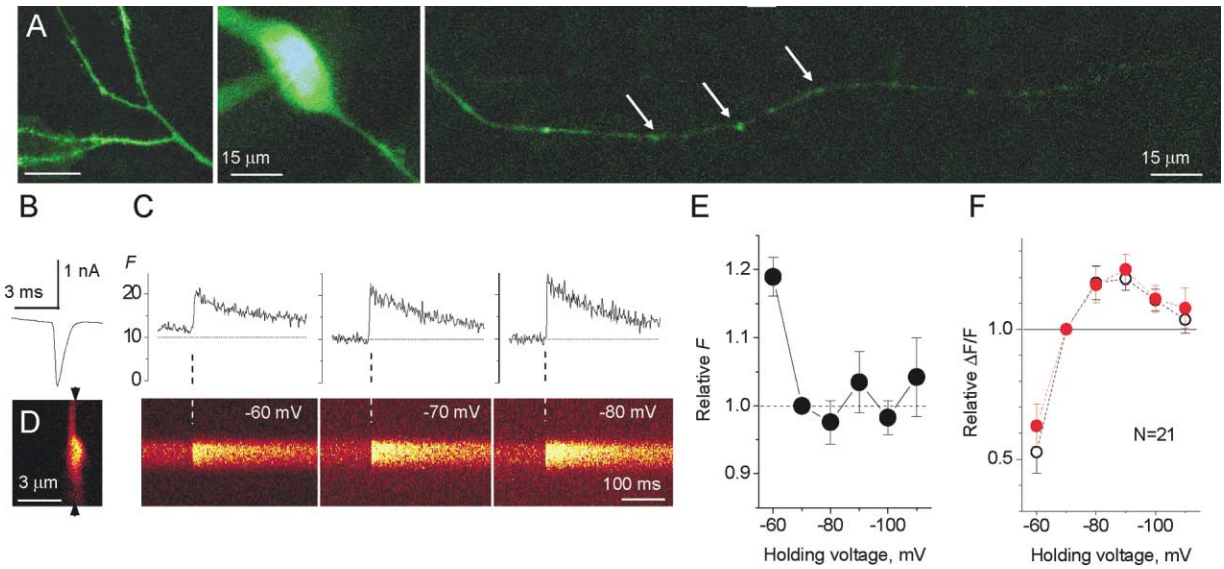

Figure 5. Biphasic Relationship between Mossy Fiber Membrane Potential and Spike-Evoked Ca^{2+} Transients in Individual Axonal Varicosities

(A) Alexa Fluor 594 fluorescence image of a granule cell (note different scales). Arrows indicate examples of axonal varicosities selected for Ca^{2+} imaging (collage of 33 images obtained with Kalman averaging at different focal depths). Scale bar equals 50 μm.

(B–D) An antidromic action potential (recorded as an AC in B) induced in an individual varicosity (shown in D) a fast Ca^{2+} transient. Example traces and line scans in (C) are averages of 10 sweeps (traces show the absolute fluorescence *F* in arbitrary units of brightness; the timescale in the line scan also applies to the traces). Varying the somatic holding voltage modulated the size of the transient (average traces are shown for illustration purposes only: $\Delta F/F$ values were calculated in each individual sweep).

(E) Summary of relationship between baseline Ca^{2+}-dependent fluorescence and somatic holding voltage V_m ($n = 21$ varicosities in 19 cells). Ordinate: data normalized to the baseline signal at $V_m = -70$ mV.

(F) Summary of relationship between the action potential-dependent fluoresence transient (expressed as $\Delta F/F$) and somatic holding potential, normalized to that seen at −70 mV (in control conditions $\Delta F/F = 31\% \pm 5\%$). The red symbols show the relationship between fluorescence transient and V_m corrected for changes in average baseline fluorescence $\langle F \rangle$ (see Experimental Procedures).

subunits are both expressed at high level in the hippocampus (Sperk et al., 1997). α_1 immunolabeling at ultrastructural resolution in mossy fiber synapses is described elsewhere (Bergersen et al., 2003). As for α_2, this subunit occurs in superficial laminae of the spinal cord (Bohlhalter et al., 1996) and at axo-axonic synapses in the forebrain (Nusser et al., 1996). At both of these locations, receptors containing α_2 subunits are candidates to mediate presynaptic inhibition. We therefore asked whether α_2 subunit-containing receptors are located presynaptically at mossy fiber synapses. Punctate immunolabeling was seen in stratum lucidum of CA3, the termination region of mossy fibers (Figures 7A and 7D; see also Sperk et al., 1997). Double labeling for α_2 and synaptophysin, a specific presynaptic marker (Wiedenmann and Franke, 1985), revealed abundant colocalization of the two epitopes (Figures 7C and 7F), consistent with a presynaptic localization of the receptors.

To probe the detailed distribution of α_2 subunits, we examined postembedding immunogold labeling at the ultrastructural level. We identified mossy fiber synapses in stratum lucidum by their large profile areas of complex shape, a large population of presynaptic pleomorphic and dense-core vesicles, and multiple postsynaptic densities contacting complex postsynaptic spines. The α_2 labeling density over mossy fiber terminals (2.34 ± 0.39 particles/μm^2) was significantly higher than background (mitochondria and myelin, 0.59 ± 0.22 particles/μm^2; $p < 0.001$, Mann-Whitney test). Immunolabeling was present at symmetrical synapses (Figure 7G) but also at mossy fiber synapses, where it was mainly found at the synaptic cleft; at extrasynaptic membranes of mossy fiber axons; in the postsynaptic spine; and at vesicular structures 70–100 nm in diameter within presynaptic terminals, often in close proximity to the cell membrane (Figures 7H–7M). Single sections showed labeling at 83% of mossy fiber synapses. Among the immunoreactive synapses, labeling was most frequently located inside the presynaptic terminals, possibly reflecting receptor trafficking. Of 96 synapses evaluated, 80 were immunolabeled. Among the immunopositive synapses, labeling was seen in the presynaptic profile in 79, in the postsynaptic profile in 41, in the synaptic cleft in 27, and at extrasynaptic membranes of the presynaptic terminal in 43. Thus, $GABA_A$ receptors containing the α_2 subunit do occur in a pattern consistent with a presynaptic location.

Discussion

The present study is the first to show that both GABA and exogenous $GABA_A$ receptor agonists can alter the function of an important excitatory cortical pathway in situ by acting on ionotropic receptors in the distal parts of the axon. This effect was mediated by $GABA_A$ receptors on mossy fibers themselves, rather than through indirect effects on the axonal microenvironment, because manipulation of $[Cl^-]$ in a single granule cell switched the effect of muscimol from decreasing to en-

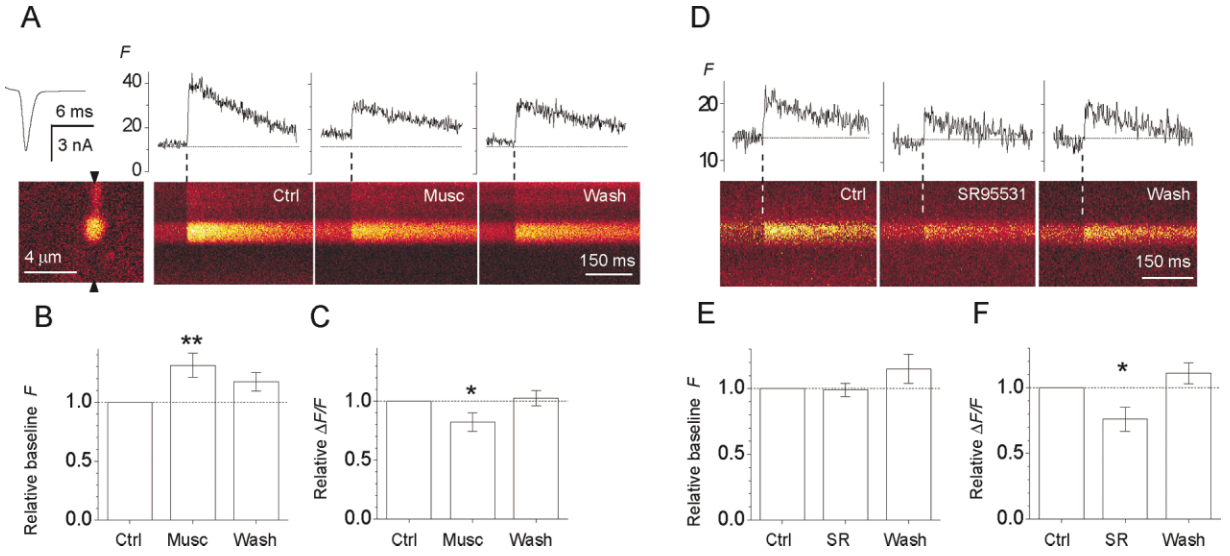

Figure 6. $GABA_A$ Receptors Modulate Spike-Evoked Ca^{2+} Transients in Individual Axonal Varicosities

(A) Example traces taken from one cell showing the effect of muscimol (1 μM) application on the baseline and incremental action potential-dependent fluorescence (average of 8–10 trials; $\Delta F/F$ values were calculated from individual sweeps).

(B and C) Summary of the effect of muscimol on the baseline fluorescence (B) and the action potential-evoked fluorescence transient (C; n = 10).

(D) Example traces showing the effect of SR95531 (10 μM) on mossy fiber Ca^{2+}-dependent fluorescence (averages of 8–10 trials).

(E and F) Summary of the effect of SR95531 on the baseline fluorescence (E) and action potential-evoked fluorescence transient (F; n = 7).

*$p < 0.05$; **$p < 0.01$. Other notations are as in Figure 5.

hancing axonal excitability. This is corroborated by light and electron microscopic evidence that presynaptic $GABA_A$ receptors occur in the presynaptic and axonal membrane. Moreover, in the experimental conditions used here, blocking $GABA_A$ receptors robustly modulated mossy fiber excitability, implying that the receptors are tonically active. $GABA_A$ receptor blockade also reversibly altered antidromic AC-evoked Ca^{2+} transients in mossy fiber varicosities, implying that both phasic and tonic $GABA_A$ receptor activation could directly affect transmitter release.

How do presynaptic $GABA_A$ receptors affect mossy fiber excitability? $GABA_A$ receptor activation raised the threshold for evoking an action potential when $[Cl^-]_i$ was low (cell-attached recordings and low $[Cl^-]$ pipette solution recordings). This would, at first sight, imply that $GABA_A$ receptors hyperpolarize the axonal membrane. This is, however, difficult to reconcile with the fact that $GABA_A$ receptor-mediated responses have been reported to be depolarizing in granule cells (Misgeld et al., 1986). Moreover, the predicted E_{GABA} from the low $[Cl^-]$ pipette solution used here, taking into account a contribution from HCO_3^- permeation, is positive to −70 mV. Finally, the Ca^{2+} imaging experiments in the present study indicate that somatic depolarization and direct activation of $GABA_A$ receptors with muscimol both increase the baseline Ca^{2+}-dependent fluorescence and decrease the action potential-dependent fluorescence transient in individual mossy fiber boutons. Thus, several lines of evidence converge on the view that, even with a low Cl^- recording solution, $GABA_A$ receptors depolarize mossy fibers. A possible explanation for the increase in axonal threshold under these circumstances is that activating $GABA_A$ receptors also shunts the electrical stimulus, possibly by decreasing the tissue resistance. Consistent with this, we observed a substantial decrease in input resistance during bath (although not local) muscimol application. (We also observed a small but significant increase in the size of the electrical artifact recorded with an extracellular electrode when $GABA_A$ receptors were blocked with picrotoxin [data not shown].)

Shunting of the electrical stimulus could occur through $GABA_A$ receptors on structures distinct from the mossy fibers. However, this does not detract from the key evidence that indicates that $GABA_A$ receptors are present on the mossy fibers themselves: raising $[Cl^-]_i$ switched the effect of $GABA_A$ receptors from decreasing to increasing axonal excitability. When $[Cl^-]_i$ was high, the shunting effect (which should be independent of altering $[Cl^-]_i$ in the recorded cell) was presumably insufficient to overcome the threshold-lowering effect of a large depolarization produced by opening $GABA_A$ receptors. Under these conditions, the mossy fibers behaved analogously to primary afferents in the spinal cord, where activation of $GABA_A$ receptors lowers the threshold for antidromic action potentials (Nicoll and Alger, 1979; Rudomin et al., 1981). Indeed, a high resting intracellular $[Cl^-]$ is thought to underlie $GABA_A$ receptor-mediated increase in afferent excitability (Curtis and Lodge, 1982).

Presynaptic depolarization mediated by $GABA_A$ receptors has distinct effects on orthodromic transmission in different parts of the CNS. In the spinal cord and posterior pituitary, it decreases evoked neurotransmitter release. Depolarization-induced inactivation of Na^+ channels plays a major role in depressing the amplitude of action potentials propagating in afferent terminals (Graham and Redman, 1994; Zhang and Jackson, 1995), although shunting of ionic currents may also play a role

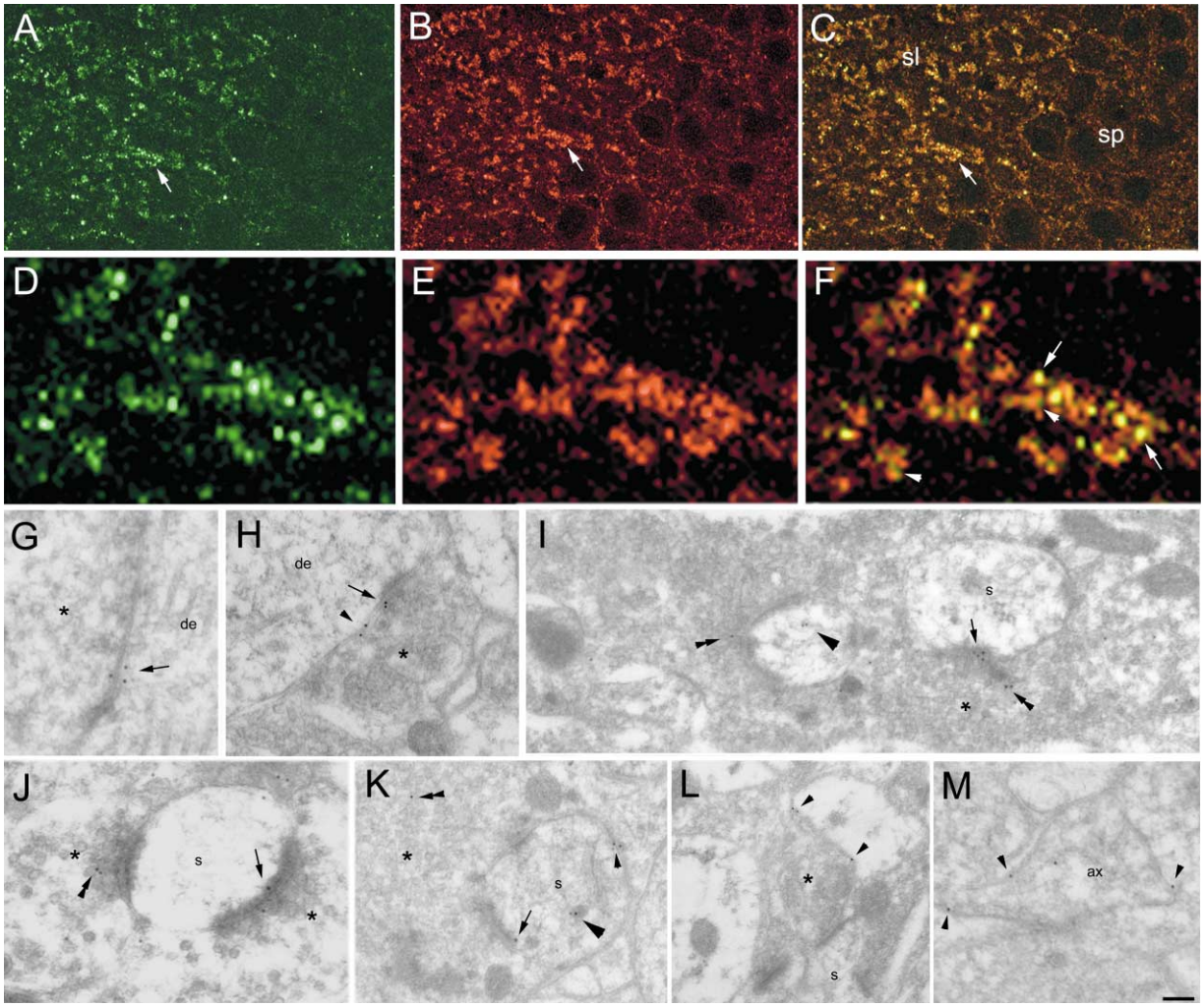

Figure 7. $GABA_A$ Receptor α_2 Subunit Immunolabeling in CA3 Stratum Lucidum of Rat Hippocampus

(A–F) Light microscopic double labeling for $GABA_A$ α_2 (green) and synaptophysin (red) demonstrates the abundance of both binding sites; sp, stratum pyramidale; sl, stratum lucidum. (D–F) Higher magnification of the area indicated by the arrows in (A)–(C), demonstrating the close apposition (arrowheads) or colocalization (arrows) of both labels. Scale bar equals 25 μm in (A)–(C) and 5 μm in (D)–(F).

(G) Electron micrograph of a gold-labeled symmetrical synapse (arrow) contacting a dendrite (de).

(H–L) Immunolabeled mossy fiber terminals. Labeling is present at the synaptic cleft (arrows), at vesicles in presynaptic terminals (double arrowheads), at extrasynaptic axonal membranes (small arrowheads), and in postsynaptic profiles (s) in close proximity to membranous structures (big arrowheads).

(M) Vesicle-containing axonal profile (ax) revealing immunolabeling at extrasynaptic membranes (arrowheads). Asterisks: presynaptic profiles; scale bar in (G) applies to other panels: (G) 80 nm; (H) 110 nm; (I) 120 nm; (J) 100 nm; (K) 160 nm; (L) 200 nm; (M) 120 nm.

both at these terminals (Segev, 1990) and in sensory afferents of the crayfish (Cattaert and El Manira, 1999). However, in the medial nucleus of the trapezoid body, presynaptic depolarization via activation of either glycine or $GABA_A$ receptors enhances evoked glutamate release (Turecek and Trussell, 2001, 2002).

In the present study, the effect of presynaptic $GABA_A$ receptors on orthodromic transmission could not be studied directly because of the confounding effects of changes in axon recruitment, GABAergic innervation of postsynaptic cells, and possible corelease of GABA with glutamate. Instead, we examined the effect of manipulating presynaptic $GABA_A$ receptors on the trigger for neurotransmitter release, action potential-evoked Ca^{2+} influx in individual mossy fiber varicosities. Surprisingly, activating $GABA_A$ receptors and blocking tonically active receptors both led to a reversible reduction in Ca^{2+} influx, as inferred from the incremental fluorescence emitted by Fluo-4. This approach suffers from the potential limitation that the axonal varicosities selected for imaging were relatively proximal, and therefore may not reflect the normal behavior of distal boutons presynaptic to CA3 pyramidal neurons, either because of intrinsic differences in the distribution and roles of $GABA_A$ receptors and Ca^{2+} channels or because they were more susceptible to experimental perturbation of homeostatic mechanisms.

Notwithstanding these limitations, the effect of activating $GABA_A$ receptors on action potential-dependent Ca^{2+} transients was qualitatively similar to that of depo-

larization. A possible mechanism is inactivation of Na^+ channels, as has been argued to occur in the spinal cord and posterior pituitary, leading to a decrease in Ca^{2+} channel opening. Interestingly, the baseline fluorescence (prior to the action potential) also increased, both when the cell body was directly depolarized and when muscimol was applied, implying that mossy fiber depolarization may have been sufficient to open low-threshold Ca^{2+} channels and/or reduce Ca^{2+} extrusion. Depolarization-induced inactivation of high-threshold Ca^{2+} channels could also play a role in reducing action potential-evoked Ca^{2+} influx.

Blocking tonically active $GABA_A$ receptors also decreased the action potential-evoked Ca^{2+} transient, although in this case there was no change in baseline fluorescence. This observation is consistent with hyperpolarization of the mossy fiber varicosity beyond the maximum in the biphasic relationship between Ca^{2+} influx and membrane potential. The absolute shape and position of this relationship with respect to membrane potential in an axonal varicosity cannot be inferred from the present study, because the degree of electrotonic attenuation along the axis is not known, and the normal resting potential of the axon may be different from that of the cell body. Nevertheless, this biphasic relationship is qualitatively consistent with the finding that progressive depolarization of mossy fibers, achieved either by raising $[K^+]_o$ or by applying increasing kainate concentrations, first increases mossy fiber EPSPs and then depresses them (Schmitz et al., 2001). (Interestingly, this biphasic relationship between EPSP amplitude and axonal depolarization was obtained with $GABA_A$ receptors blocked.) The mechanisms underlying depression of Ca^{2+} influx and transmitter release at very hyperpolarized levels approaching E_K (approximately -104 mV) are unclear, but may involve de-inactivation of K^+ channels.

The role of $GABA_A$ receptors in modulating mossy fiber function could also depend on activity-dependent changes in E_{GABA}. Thus, intense GABA release in the vicinity of a mossy fiber could cause intracellular Cl^- accumulation, which could both depolarize the $GABA_A$ reversal potential and contribute to further depolarization by engendering HCO_3^- and K^+ efflux (Voipio and Kaila, 2000). Conversely, mossy fiber depolarization mediated by kainate receptor activation and/or I_h enhancement, as have been proposed to contribute to use-dependent facilitation and LTP (Schmitz et al., 2001; Lauri et al., 2001; Mellor et al., 2002; although see Chevaleyre and Castillo, 2002), might render $GABA_A$ receptors less depolarizing. The effect of GABA release from neighboring neurons on transmitter release could therefore depend on the activity history of the target mossy fiber.

Mossy fiber excitability was modulated by zolpidem. This distinguishes the receptors on mossy fibers from extrasynaptic $GABA_A$ receptors mediating tonic inhibition of granule cells (Nusser and Mody, 2002). Although benzodiazepine sensitivity is conventionally associated with relatively low-affinity $GABA_A$ receptors, diazepam can enhance GABAergic currents at sub- or low-micromolar GABA (Eghbali et al., 1997). The immunolabeling reported here implies that α_2 is expressed in mossy fibers. Although this is consistent with the effect of zolpidem (which has been reported to displace Ro15-1788 from α_2 subunit-containing receptors with a K_i of 0.4 μM; Pritchett and Seeburg, 1990), the full subunit composition of the receptors at mossy fibers remains to be determined. Moreover, it will be important to explore the developmental expression of these subunits, not least because the immunohistochemical data reported here were obtained in adult rats.

Taken together with recent work on kainate receptors (Contractor et al., 2001; Kamiya and Ozawa, 2000; Lauri et al., 2001; Schmitz et al., 2001), the present results suggest a surprisingly rich complexity of signal integration in mossy fibers: by detecting the release of both glutamate and GABA via ionotropic receptors, these axons may rapidly integrate the activity of surrounding neurons, a function normally associated with dendrites.

Experimental Procedures

Electrophysiology

Transverse hippocampal slices (350 μm thick) were obtained from 3- to 4-week-old guinea pigs and were stored in an interface chamber for at least 1 hr prior to transfer to a submersion recording chamber. The storage and perfusion solution contained (in mM) NaCl (119), KCl (2.5), $MgSO_4$ (1.3), $CaCl_2$ (2.5), $NaHCO_3$ (26.2), NaH_2PO_4 (1), and glucose (11) and was gassed with 95% O_2/5% CO_2 (23°C–25°C). Whole-cell recordings were made from dentate granule cells under infrared differential interference contrast imaging. The following drugs were used to block AMPA, kainate, NMDA, and $GABA_B$ receptors: NBQX (50 μM), D-2-amino-5-phosphonovalerate (APV, 50 μM), and CGP52432 (5 μM). Whole-cell pipettes used to record antidromic action currents contained (in mM) Kgluconate (135), NaCl (8), HEPES (10), EGTA (0.2), MgATP (2), and Na_3GTP (0.3) (pH 7.2, osmolarity 295 mOsm). In some experiments, $KmeSO_4$ replaced Kgluconate with indistinguishable results. In the high $[Cl^-]$ solution, 145 mM KCl replaced Kgluconate and NaCl. Extracellular stimuli used to evoke antidromic or orthodromic action potentials were delivered via a monopolar electrode positioned in stratum lucidum between 500 and 1500 μm from the granule cell (stimulus duration: 500 μs, interval 2–10 s). Conditioning trains were delivered via a second electrode positioned in stratum radiatum. Local pressure application of muscimol (2.5 μM in control perfusion solution) was delivered via a patch pipette connected to a Picospritzer (General Valve Corporation, 5–10 ms, 5–20 PSI). The pipette was positioned in stratum lucidum under visual control within 50 μm of the stimulating electrode, and the bath perfusion was arranged to keep the granule cell body upstream of this position. Currents were acquired with an Axopatch 1D amplifier (Axon Instruments), and records were filtered at 1 kHz, digitized at 2–5 kHz, and stored on a personal computer. The access and input resistances were monitored throughout the experiments using a voltage step. The access resistance was <20 MΩ, and results were discarded if it changed by more than 20%. Junction potentials were not corrected. AC success rates were calculated from 6–12 trials per plotted point. Statistical comparisons were made using Student's paired or unpaired t test (without normalizing), where appropriate. Drugs were obtained from Tocris Cookson or Sigma.

Fast Ca^{2+} Imaging

For Ca^{2+} transient measurements, hippocampal slices were perfused with a solution containing (in mM) NaCl (119), KCl (2.5), $MgSO_4$ (1), $CaCl_2$ (2 or 2.5), $NaHCO_3$ (26.2), NaH_2PO_4 (1), Trolox (0.1), and glucose (11) and gassed with 95% O_2/5% CO_2 (23°C–25°C). Granule cells were recorded in whole-cell mode using a pipette solution containing (in mM): $KmeSO_4$ (135), HEPES (10), Na phosphocreatine (10), $MgCl_2$ (4), Na_2ATP (4), Na_3GTP (0.4), Alexa Fluor 594 (0.04), and Fluo-4 (0.2). Glutamate receptors were blocked as in the electrophysiology experiments. Alexa Fluor 594 was used in some experiments to help identify the mossy fiber and its varicosities, while Fluo-4 was used as the high-affinity Ca^{2+} indicator (K_d = 345 nm). Both dyes were simultaneously excited in two-photon mode at 810 nm using a femtosecond pulsed laser (SpectraPhysics MaiTai) opti-

cally linked to a confocal scanhead (BioRad, Radiance 2000) (Rusakov and Fine, 2003). Epifluorescence was collected through a 700SP filter and chromatically separated at 560 nm using a dichroic mirror that directed the two emission signals into separate photomultiplier tubes ($\lambda_m < 560$ nm for Fluo-4 and 560 nm $< \lambda_m <$ 700 nm for Alexa 594). Large axonal varicosities were traced along the granule cell axon 70–200 μm from the soma. Line scanning (at 500 Hz) was run for a sweep duration of 600 ms at approximately 30 s intervals. A single antidromic action current was evoked using an extracellular bipolar electrode, 150 ms after the scanning sweep onset.

Data acquisition was only started once the baseline fluorescence had stabilized (15–20 min following break-in) to ensure that the indicator concentration was constant, and the varicosity was refocused every 2–3 sweeps during the course of the experiment to obtain the brightest image. The effect of somatic de- or hyperpolarization on the evoked fluorescence transient was tested by systematically changing the holding voltage, in 10 mV steps, every 5–10 sweeps, to eliminate any nonspecific drift in the fluorescence response. In some experiments, orthodromic action potentials were induced by a 5 ms voltage command step applied through the patch pipette at the granule cell body. Imaging data obtained with ortho- and antidromic propagation of action potentials were indistinguishable and therefore combined. In experiments with SR95531 and muscimol, 8–15 sweeps were recorded for each experimental condition and, to minimize photodamage, 5–6 min was allowed to lapse before scanning resumed after the drug was washed in or out. Line scans were collected as stacks of 8-bit images and analyzed offline with custom NIH Image macros. The Ca^{2+}-dependent fluorescence transient $\Delta F/F$ was calculated within each sweep from the fluorescence signals (collected across the imaged varicosity) integrated over 100 ms time windows before and after the onset of the action current, which was simultaneously recorded. The average signal within each experimental phase $\langle \Delta F/F \rangle$ (e.g., at a fixed value of V_m or during control/wash-in/wash-out) was then calculated. To assess the baseline fluorescence changes between experimental phases, we also calculated the average fluorescence $\langle F \rangle$ within each experimental phase. Because changes in $\langle F \rangle$ resulting from experimental manipulations could affect the interpretation of $\Delta F/F$, we weighted $\langle \Delta F/F \rangle$ values by $\langle F \rangle$. The rationale for this correction factor is detailed as follows.

Baseline Fluorescence Correction Factor

Kinetic equations predict a simple relationship between free and buffer bound Ca^{2+} ($[Ca^{2+}]$ and $[CaB]$, respectively) in steady-state conditions:

$$[CaB] = \frac{[Ca^{2+}][B_i]_{tot}}{([Ca^{2+}] + K'_d)}, \quad (1)$$

where K'_d is the dissociation constant of the i^{th} buffer/indicator, and $[B_i]_{tot}$ is its total concentration. Recast in terms of fluorescence, this transforms into (Tsien, 1989)

$$\frac{[Ca^{2+}]}{K'_d} = \frac{F - F_{min}}{F_{max} - F}, \quad (2)$$

where F_{min}, F, and F_{max} are, respectively, the residual (Ca-free), observed, and maximum (Ca-saturated) fluorescence of the indicator. In the case of Fluo-4, $K_d \sim 0.4$ μM and $F \gg F_{min}$. Jackson and Redman (2003) have estimated the resting free $[Ca^{2+}]$ in the mossy fiber terminals at ~74 nM. When substituted into expression 2, this corresponds to a Fluo-4 F_{max}/F ratio, hereafter denoted ϕ, between 6 and 7. Our preliminary measurements of F_{max} with trains of stimuli are consistent with this.

When the high-affinity endogenous buffer *EB* and fluorescence indicator *FI* are both present in the terminal, the total quasi steady-state Ca^{2+} concentration $[Ca]_{tot}$ is

$$[Ca]_{tot} = [Ca^{2+}] + [CaFI] + [CaEB], \quad (3)$$

where the last two terms correspond to the Ca bound indicator and Ca bound buffer, respectively. This expression can be recast using equations 1 and 2:

$$[Ca]_{tot} = K_d^{FI} \frac{1}{1 - \phi} + [FI]_{tot} \frac{1}{\phi} + [EB]_{tot} \frac{1}{\phi^{EB}}, \quad (4)$$

where K_d^{FI} is the dissociation constant of *FI*, and $\phi^{EB} = 1 + K_d^{EB}/[Ca^{2+}]$, where K_d^{EB} is the dissociation constant of *EB*. Jackson and Redman (2003) have estimated $[EB]_{tot} = 130$ μM, $K_d^{EB} = 500$ nM, and therefore $\phi^{EB} = 7.75$.

Because F_{max} is a constant, expression 4 can be used to directly relate an increment in total Ca^{2+} (that is, total Ca^{2+} influx) to a percentage change in the fluorescence F.

In our voltage dependence experiments (Figure 5C), the average $\Delta F/F$ signal was 35% ± 4%, and in the muscimol experiments (Figure 6A) it was 34% ± 7%. The observed increases in the baseline fluorescence in these experiments were 20%–30% (Figures 5 and 6). Given the concentration values listed above and given the predicted range of ϕ between 6 and 7, it follows from expression 4 that in the presence of a baseline F increase of 30%, the same $\Delta F/F$ corresponds to a 30% ± 3% higher Ca^{2+} influx. In other words, weighting $\langle \Delta F/F \rangle$ values by $\langle F \rangle$ provided a correction with >90% accuracy in the average conditions of the experiments.

Although nonspecific photodamage in our experiments (30–45 sweeps, 600 ms long) is unlikely to exceed 5%–7% (Koester et al., 1999), individual boutons tended to show a small increase in the baseline fluorescence toward the end of the experiment (see, for instance, Figures 6B and 6E). Whenever such increases exceeded 30% (after washout of drugs), the data were discarded. Within individual sweeps, photo-bleaching was less than 2%.

Light Microscopic Immunohistochemistry

Vibratome sections were obtained from two adult male Sprague Dawley rats. Animals were anesthetized with urethane (1.5 g/kg, i.p.) and perfused over 20 min with 200 ml of 4% paraformaldehyde in 0.1 M phosphate buffer (pH 7.2) (PB). After dissection, brains were embedded in 7% Agarose, and 30 μm vibratome sections were cut transversely through the hippocampus. Sections were collected in 1% glycine/PB, washed in PB (3 × 10 min), and blocked for 30 min in incubation medium (IM) consisting of 10% fetal calf serum and 1% bovine serum albumin in PB; 0.1% saponin was added to permeabilize the tissue. Sections were then incubated overnight at 4°C in the presence of both primary antibodies (goat anti-$GABA_A$ α_2, Santa Cruz # sc-7350; mouse anti-synaptophysin, Boehringer Mannheim SY38), each diluted 1:100 in IM with 0.01% saponin. After extensive rinsing in PB (7 × 1 hr), preparations were blocked and permeabilized as above and secondary antibodies (Alexa 488 donkey anti-goat, Molecular Probes # A-11055, dilution 1:200; Cy3 goat anti-mouse, Jackson Immunoresearch # 111-165-003, dilution 1:500) were applied in IM overnight at 4°C. After final rinsing in PB (7 × 1 hr), preparations were mounted in Mowiol 4-88 (475904, Calbiochem) and polymerized overnight at 4°C. Preparations were examined using a Leica TCS NT confocal microscope.

EM-Immunogold Labeling Experiments

Ultrathin sections were obtained from freeze-substituted hippocampal tissue of two adult CFHB male rats as described previously (Fabian-Fine et al., 2001). Ultrathin sections (50 nm) were cut with a Reichert Ultracut and collected on pioloform-coated single-slot nickel grids. Grids were then mounted in a grid support plate, soaked in PB for 30 min, and preincubated in IM for 30 min at room temperature. Sections were then incubated with goat anti-$GABA_A$ α_2 antibody (see above; 1:100 in IM) overnight at 4°C. After thorough washing (4 × 10 min in PB) and preincubation in IM (30 min), the secondary antibody (rabbit anti-goat IgG coupled to 10 nm gold particles; Sigma G-5402) was applied at a dilution of 1:100 in IM for 4 hr at 37°C. Preparations were washed subsequently in PB (5 × 10 min) before final rinsing in double-distilled water. The sections were contrasted with uranyl acetate (4 min) and Reynold's lead citrate (50 s) according to standard EM methods. Preparations were examined using a Philips 201C electron microscope, and mossy fiber synapses were identified as described previously (Reid et al., 2001). Control preparations from which the primary antibody was omitted showed no signal. Immunolabeling was analyzed over mossy fiber synapses randomly selected at low magnification. Gold particles were counted at high magnification, and their density within synaptic profiles de-

termined using NIH Image. Synapses were only scored as immunopositive when the labeling was above background level (evaluated over areas where no staining was expected, e.g., mitochondria and myelin).

Acknowledgments

We are grateful to Drs. Hugh Bostock, Alan Fine, and Barrie Lancaster for comments on the manuscript. This work was supported by the Medical Research Council, the Brain Research Trust, the Wellcome Trust, and the Killam Trust.

Received: December 2, 2002
Revised: July 31, 2003
Accepted: August 20, 2003
Published: September 10, 2003

References

Avoli, M., Methot, M., and Kawasaki, H. (1998). GABA-dependent generation of ectopic action potentials in the rat hippocampus. Eur. J. Neurosci. *10*, 2714–2722.

Bergerson, L., Ruiz, A., Bjaalie, J.G., Kullmann, D.M., and Gundersen, V. (2003). GABA and $GABA_A$ receptors at hippocampal mossy fibre synapses. Eur. J. Neurosci. *18*, 931–941.

Bohlhalter, S., Weinmann, O., Mohler, H., and Fritschy, J.M. (1996). Laminar compartmentalization of GABAA-receptor subtypes in the spinal cord: an immunohistochemical study. J. Neurosci. *16*, 283–297.

Cattaert, D., and El Manira, A. (1999). Shunting versus inactivation: analysis of presynaptic inhibitory mechanisms in primary afferents of the crayfish. J. Neurosci. *19*, 6079–6089.

Chevaleyre, V., and Castillo, P.E. (2002). Assessing the role of Ih channels in synaptic transmission and mossy fiber LTP. Proc. Natl. Acad. Sci. USA *99*, 9538–9543.

Contractor, A., Swanson, G., and Heinemann, S.F. (2001). Kainate receptors are involved in short- and long-term plasticity at mossy fiber synapses in the hippocampus. Neuron *29*, 209–216.

Cox, C.L., Denk, W., Tank, D.W., and Svoboda, K. (2000). Action potentials reliably invade axonal arbors of rat neocortical neurons. Proc. Natl. Acad. Sci. USA *97*, 9724–9728.

Curtis, D.R., and Lodge, D. (1982). The depolarization of feline ventral horn group Ia spinal afferent terminations by GABA. Exp. Brain Res. *46*, 215–233.

Debanne, D., Guerineau, N.C., Gahwiler, B.H., and Thompson, S.M. (1997). Action-potential propagation gated by an axonal I(A)-like K+ conductance in hippocampus. Nature *389*, 286–289.

Ebert, B., Thompson, S.A., Saounatsou, K., McKernan, R., Krogsgaard-Larsen, P., and Wafford, K.A. (1997). Differences in agonist/antagonist binding affinity and receptor transduction using recombinant human gamma-aminobutyric acid type A receptors. Mol. Pharmacol. *52*, 1150–1156.

Eccles, J.C., Schmidt, R.F., and Willis, W.D. (1963). Pharmacological studies of presynaptic inhibition. J. Physiol. *168*, 500–530.

Eghbali, M., Curmi, J.P., Birnir, B., and Gage, P.W. (1997). Hippocampal GABA(A) channel conductance increased by diazepam. Nature *388*, 71–75.

Emptage, N.J., Reid, C.A., and Fine, A. (2001). Calcium stores in hippocampal synaptic boutons mediate short-term plasticity, store-operated Ca^{2+} entry, and spontaneous transmitter release. Neuron *29*, 197–208.

Fabian-Fine, R., Skehel, P., Errington, M.L., Davies, H.A., Sher, E., Stewart, M.G., and Fine, A. (2001). Ultrastructural distribution of the alpha7 nicotinic acetylcholine receptor subunit in rat hippocampus. J. Neurosci. *21*, 7993–8003.

Fassio, A., Rossi, F., Bonanno, G., and Raiteri, M. (1999). GABA induces norepinephrine exocytosis from hippocampal noradrenergic axon terminals by a dual mechanism involving different voltage-sensitive calcium channels. J. Neurosci. Res. *57*, 324–331.

Fung, S.C., and Fillenz, M. (1983). The role of pre-synaptic GABA and benzodiazepine receptors in the control of noradrenaline release in rat hippocampus. Neurosci. Lett. *42*, 61–66.

Geiger, J.R., and Jonas, P. (2000). Dynamic control of presynaptic Ca(2+) inflow by fast-inactivating K(+) channels in hippocampal mossy fiber boutons. Neuron *28*, 927–939.

Graham, B., and Redman, S. (1994). A simulation of action potentials in synaptic boutons during presynaptic inhibition. J. Neurophysiol. *71*, 538–549.

Gutierrez, R., and Heinemann, U. (2001). Kindling induces transient fast inhibition in the dentate gyrus-CA3 projection. Eur. J. Neurosci. *13*, 1371–1379.

Henze, D.A., Urban, N.N., and Barrionuevo, G. (2000). The multifarious hippocampal mossy fiber pathway: a review. Neuroscience *98*, 407–427.

Jackson, M.B., and Redman, S.J. (2003). Calcium dynamics, buffering, and buffer saturation in the boutons of dentate granule-cell axons in the hilus. J. Neurosci. *23*, 1612–1621.

Jang, I.S., Jeong, H.J., and Akaike, N. (2001). Contribution of the Na-K-Cl cotransporter on GABA(A) receptor-mediated presynaptic depolarization in excitatory nerve terminals. J. Neurosci. *21*, 5962–5972.

Kaila, K., Voipio, J., Paalasmaa, P., Pasternack, M., and Deisz, R.A. (1993). The role of bicarbonate in GABAA receptor-mediated IPSPs of rat neocortical neurones. J. Physiol. *464*, 273–289.

Kamiya, H., and Ozawa, S. (2000). Kainate receptor-mediated presynaptic inhibition at the mouse hippocampal mossy fibre synapse. J. Physiol. (Lond.) *523*, 653–665.

Kamiya, H., Shinozaki, H., and Yamamoto, C. (1996). Activation of metabotropic glutamate receptor type 2/3 suppresses transmission at rat hippocampal mossy fibre synapses. J. Physiol. (Lond.) *493*, 447–455.

Koester, H.J., and Sakmann, B. (2000). Calcium dynamics associated with action potentials in single nerve terminals of pyramidal cells in layer 2/3 of the young rat neocortex. J. Physiol. *529*, 625–646.

Koester, H.J., Baur, D., Uhl, R., and Hell, S.W. (1999). Ca^{2+} fluorescence imaging with pico- and femtosecond two-photon excitation: signal and photodamage. Biophys. J. *77*, 2226–2236.

Lanthorn, T.H., Ganong, A.H., and Cotman, C.W. (1984). 2-amino-4-phosphonobutyrate selectively blocks mossy fiber-CA3 responses in guinea pig but not rat hippocampus. Brain Res. *290*, 174–178.

Lauri, S.E., Bortolotto, Z.A., Bleakman, D., Ornstein, P.L., Lodge, D., Isaac, J.T., and Collingridge, G.L. (2001). A critical role of a facilitatory presynaptic kainate receptor in mossy fiber LTP. Neuron *32*, 697–709.

Lukasiewicz, P.D., and Werblin, F.S. (1994). A novel GABA receptor modulates synaptic transmission from bipolar to ganglion and amacrine cells in the tiger salamander retina. J. Neurosci. *14*, 1213–1223.

Mellor, J., Nicoll, R.A., and Schmitz, D. (2002). Mediation of hippocampal mossy fiber long-term potentiation by presynaptic Ih channels. Science *295*, 143–147.

Min, M.Y., Rusakov, D.A., and Kullmann, D.M. (1998). Activation of AMPA, kainate, and metabotropic receptors at hippocampal mossy fiber synapses: role of glutamate diffusion. Neuron *21*, 561–570.

Misgeld, U., Deisz, R.A., Dodt, H.U., and Lux, H.D. (1986). The role of chloride transport in postsynaptic inhibition of hippocampal neurons. Science *232*, 1413–1415.

Nicoll, R.A., and Alger, B.E. (1979). Presynaptic inhibition: transmitter and ionic mechanisms. Int. Rev. Neurobiol. *21*, 217–258.

Nusser, Z., and Mody, I. (2002). Selective modulation of tonic and phasic inhibitions in dentate gyrus granule cells. J. Neurophysiol. *87*, 2624–2628.

Nusser, Z., Sieghart, W., Benke, D., Fritschy, J.M., and Somogyi, P. (1996). Differential synaptic localization of two major gamma-aminobutyric acid type A receptor alpha subunits on hippocampal pyramidal cells. Proc. Natl. Acad. Sci. USA *93*, 11939–11944.

Overstreet, L.S., and Westbrook, G.L. (2001). Paradoxical reduction of synaptic inhibition by vigabatrin. J. Neurophysiol. *86*, 596–603.

Payne, J.A., Stevenson, T.J., and Donaldson, L.F. (1996). Molecular characterization of a putative K-Cl cotransporter in rat brain. A neuronal-specific isoform. J. Biol. Chem. *271*, 16245–16252.

Pouzat, C., and Marty, A. (1999). Somatic recording of GABAergic autoreceptor current in cerebellar stellate and basket cells. J. Neurosci. *19*, 1675–1690.

Pritchett, D.B., and Seeburg, P.H. (1990). Gamma-aminobutyric acidA receptor alpha 5-subunit creates novel type II benzodiazepine receptor pharmacology. J. Neurochem. *54*, 1802–1804.

Reid, C.A., Fabian-Fine, R., and Fine, A. (2001). Postsynaptic calcium transients evoked by activation of individual hippocampal mossy fiber synapses. J. Neurosci. *21*, 2206–2214.

Rudomin, P., Engberg, I., and Jimenez, I. (1981). Mechanisms involved in presynaptic depolarization of group I and rubrospinal fibers in cat spinal cord. J. Neurophysiol. *46*, 532–548.

Rusakov, D.A., and Fine, A. (2003). Extracellular Ca^{2+} depletion contributes to fast activity-dependent modulation of synaptic transmission in the brain. Neuron *37*, 287–297.

Sabatini, B.L., and Svoboda, K. (2000). Analysis of calcium channels in single spines using optical fluctuation analysis. Nature *408*, 589–593.

Sandler, R., and Smith, A.D. (1991). Coexistence of GABA and glutamate in mossy fiber terminals of the primate hippocampus: an ultrastructural study. J. Comp. Neurol. *303*, 177–192.

Saridaki, E., Carter, D.A., and Lightman, S.L. (1989). Gamma-aminobutyric acid regulation of neurohypophysial hormone secretion in male and female rats. J. Endocrinol. *121*, 343–349.

Scanziani, M., Salin, P.A., Vogt, K.E., Malenka, R.C., and Nicoll, R.A. (1997). Use-dependent increases in glutamate concentration activate presynaptic metabotropic glutamate receptors. Nature *385*, 630–634.

Schmitz, D., Mellor, J., and Nicoll, R.A. (2001). Presynaptic kainate receptor mediation of frequency facilitation at hippocampal mossy fiber synapses. Science *291*, 1972–1976.

Segev, I. (1990). Computer study of presynaptic inhibition controlling the spread of action potentials into axonal terminals. J. Neurophysiol. *63*, 987–998.

Sloviter, R.S., Dichter, M.A., Rachinsky, T.L., Dean, E., Goodman, J.H., Sollas, A.L., and Martin, D.L. (1996). Basal expression and induction of glutamate decarboxylase and GABA in excitatory granule cells of the rat and monkey hippocampal dentate gyrus. J. Comp. Neurol. *373*, 593–618.

Sperk, G., Schwarzer, C., Tsunashima, K., Fuchs, K., and Sieghart, W. (1997). GABA(A) receptor subunits in the rat hippocampus I: immunocytochemical distribution of 13 subunits. Neuroscience *80*, 987–1000.

Stasheff, S.F., Mott, D.D., and Wilson, W.A. (1993). Axon terminal hyperexcitability associated with epileptogenesis in vitro. II. Pharmacological regulation by NMDA and GABAA receptors. J. Neurophysiol. *70*, 976–984.

Stell, B.M., and Mody, I. (2002). Receptors with different affinities mediate phasic and tonic GABA(A) conductances in hippocampal neurons. J. Neurosci. *22*, RC223.

Tachibana, M., and Kaneko, A. (1987). Gamma-aminobutyric acid exerts a local inhibitory action on the axon terminal of bipolar cells: evidence for negative feedback from amacrine cells. Proc. Natl. Acad. Sci. USA *84*, 3501–3505.

Tsien, R.Y. (1989). Fluorescent probes for cell signaling. Annu. Rev. Neurosci. *12*, 227–253.

Turecek, R., and Trussell, L.O. (2001). Presynaptic glycine receptors enhance transmitter release at a mammalian central synapse. Nature *411*, 587–590.

Turecek, R., and Trussell, L.O. (2002). Reciprocal developmental regulation of presynaptic ionotropic receptors. Proc. Natl. Acad. Sci. USA *99*, 13884–13889.

Verdier, D., Lund, J.P., and Kolta, A. (2003). GABAergic control of action potential propagation along axonal branches of mammalian sensory neurons. J. Neurosci. *23*, 2002–2007.

Vignes, M., Clarke, V.R., Parry, M.J., Bleakman, D., Lodge, D., Ornstein, P.L., and Collingridge, G.L. (1998). The GluR5 subtype of kainate receptor regulates excitatory synaptic transmission in areas CA1 and CA3 of the rat hippocampus. Neuropharmacology *37*, 1269–1277.

Vogt, K.E., and Nicoll, R.A. (1999). Glutamate and gamma-aminobutyric acid mediate a heterosynaptic depression at mossy fiber synapses in the hippocampus. Proc. Natl. Acad. Sci. USA *96*, 1118–1122.

Voipio, J., and Kaila, K. (2000). GABAergic excitation and K(+)-mediated volume transmission in the hippocampus. Prog. Brain Res. *125*, 329–338.

Walker, M.C., Ruiz, A., and Kullmann, D.M. (2001). Monosynaptic gabaergic signaling from dentate to ca3 with a pharmacological and physiological profile typical of mossy fiber synapses. Neuron *29*, 703–715.

Weisskopf, M.G., Zalutsky, R.A., and Nicoll, R.A. (1993). The opioid peptide dynorphin mediates heterosynaptic depression of hippocampal mossy fibre synapses and modulates long-term potentiation. Nature *362*, 423–427.

Wiedenmann, B., and Franke, W.W. (1985). Identification and localization of synaptophysin, an integral membrane glycoprotein of Mr 38,000 characteristic of presynaptic vesicles. Cell *41*, 1017–1028.

Yamamoto, C., Sawada, S., and Takada, S. (1983). Suppressing action of 2-amino-4-phosphonobutyric acid on mossy fiber-induced excitation in the guinea pig hippocampus. Exp. Brain Res. *51*, 128–134.

Yokoi, M., Kobayashi, K., Manabe, T., Takahashi, T., Sakaguchi, I., Katsuura, G., Shigemoto, R., Ohishi, H., Nomura, S., Nakamura, K., et al. (1996). Impairment of hippocampal mossy fiber LTD in mice lacking mGluR2. Science *273*, 645–647.

Zhang, S.J., and Jackson, M.B. (1993). GABA-activated chloride channels in secretory nerve endings. Science *259*, 531–534.

Zhang, S.J., and Jackson, M.B. (1995). GABAA receptor activation and the excitability of nerve terminals in the rat posterior pituitary. J. Physiol. *483*, 583–595.